Drug-target Mendelian randomization analysis supports lowering plasma ANGPTL3, ANGPTL4, and APOC3 levels as strategies for reducing cardiovascular disease risk

Fredrik Landfors[1, 2, *], Stefan K. Nilsson[2, 3], Sander Kersten[4, 5]

[1] Department of Public Health and Clinical Medicine, Section of Medicine, Umea University, S-901 87 Umea, Sweden.

[2] Lipigon Pharmaceuticals AB, S-907 36 Umea, Sweden.

[3] Department of Medical Biosciences, Umea University, S-901 87 Umea, Sweden.

[4] Nutrition, Metabolism, and Genomics group, Division of Human Nutrition and Health, Wageningen University, 6708WE, Wageningen, the Netherlands.

[5] Division of Nutritional Sciences, Cornell University, Ithaca, NY 14853, USA.

[*] To whom correspondence should be addressed.

Contact information for the corresponding author: Fredrik Landfors, Department of Public Health and Clinical Medicine, Umea University, S-901 87 Umea, Sweden; Email: Fredrik.Landfors@umu.se; Phone: +46 (0) 70-454 92 08.

ABSTRACT

Background and Aims: APOC3, ANGPTL3, and ANGPTL4 are circulating proteins that are actively pursued as pharmacological targets to treat dyslipidemia and reduce the risk of atherosclerotic cardiovascular disease. Here, we used human genetic data to compare the predicted therapeutic and adverse effects of APOC3, ANGPTL3, and ANGPTL4 inactivation.

Methods: We conducted drug-target Mendelian randomization analyses using variants in proximity to the genes associated with circulating protein levels to compare APOC3, ANGPTL3, and ANGPTL4 as drug targets. We obtained exposure and outcome data from large-scale genome-wide association studies and used generalized least squares to correct for linkage disequilibrium-related correlation. We evaluated six primary cardiometabolic endpoints and screened for potential side effects across 694 disease-related endpoints, 43 clinical laboratory tests, and 11 internal organ MRI measurements.

Results: Genetically lowering circulating ANGPTL4 levels reduced the odds of coronary artery disease (CAD) (odds ratio, 0.57 per s.d. protein [95%CI,0.47–0.70]) and type 2 diabetes (T2D) (odds ratio, 0.73 per s.d. protein [95%CI,0.57–0.94]). Genetically lowering circulating APOC3 levels also reduced the odds of CAD (odds ratio, 0.90 per s.d. protein [95%CI,0.82–0.99]). Genetically lowered ANGPTL3 levels via common variants were not associated with CAD. However, meta-analysis of loss-of-function variants revealed that *ANGPTL3* inactivation protected against CAD (odds ratio, 0.71 per allele [95%CI,0.62–0.82]). Analysis of lowered ANGPTL3, ANGPTL4, and APOC3 levels did not identify important safety concerns.

Conclusion: Human genetic evidence suggests that therapies aimed at reducing circulating levels of ANGPTL3, ANGPTL4, and APOC3 reduce the risk of CAD. ANGPTL4 lowering may also reduce the risk of T2D.

STRUCTURED GRAPHICAL ABSTRACT

Key Question: Does human genetics support that triglyceride-lowering drugs targeting ANGPTL3, ANGPTL4, and APOC3 will reduce the risk of cardiometabolic disease without causing side effects?

Key Finding: Genetically lowered circulating ANGPTL4 reduced coronary artery disease and type 2 diabetes risk. Genetically lowered ANGPTL3 and APOC3 also reduced coronary artery disease risk, but no impact on type 2 diabetes risk was observed.

Take-home Message: Human genetics suggest that ANGPTL3, ANGPTL4, and APOC3-lowering medications may prevent CAD. Medicines targeting ANGPTL4 may have added benefits for patients with type 2 diabetes.

Study design

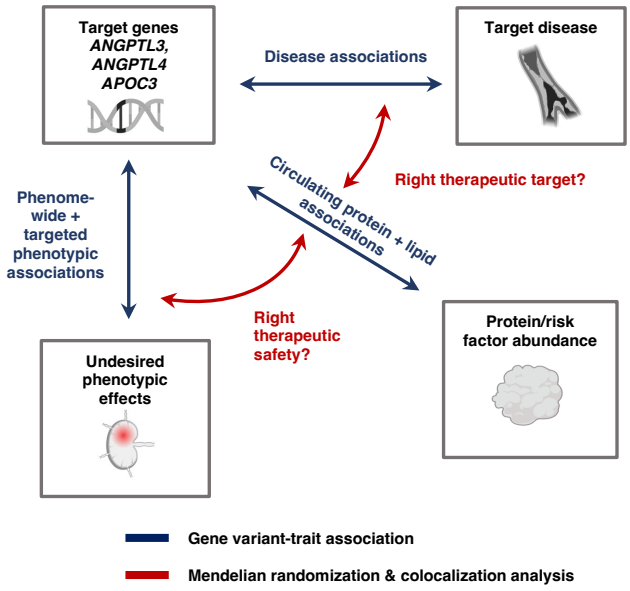

Key findings

		ANGPTL4	*ANGPTL3*	*APOC3*
Cardio-metabolic Disease	Chronic kidney disease	–	–	–
	Coronary artery disease	Improves	Improves	Improves
	Ischemic stroke	–	–	–
	Type 2 diabetes	Improves	–	–
	Non-alcoholic fatty liver disease	–	–	–
Safety	Routine labs	Weak	Weak	Weak
	Imaging	–	–	–
	Lymphadeno-pathies	–		
	Phenome-wide association study	Improves ASCVD and T2D outcomes		

Graphical abstract summarizing the study's methodology and findings.
A: Graphical abstract summarizing the overall study design. **B:** A summary of the results categorized into three groups. The term 'improves' denotes a statistically significant association with a clinically relevant effect magnitude. The term 'weak' refers to a statistically significant association with no clinically significant effect. 'ASCVD' denotes atherosclerotic cardiovascular disease. 'T2D' denotes type 2 diabetes.

INTRODUCTION

APOC3, ANGPTL3, and ANGPTL4 are circulating proteins that regulate plasma cholesterol and triglyceride (TG) levels. They mainly act by inhibiting the enzyme lipoprotein lipase. All three proteins are actively pursued as pharmacological targets to treat dyslipidemia and reduce the risk of atherosclerotic cardiovascular disease. The inactivation of APOC3 using ASOs (Volanesorsen, Olezarsen) has been shown to substantially reduce plasma TG levels in different patient groups with severe hypertriglyceridemia (1). Volanesorsen is a second-generation ASO that was approved in Europe for treating familial chylomicronemia syndrome. Olezarsen is a third-generation ASO that very recently received fast-track designation from the FDA. Currently, several human trials are ongoing with an RNAi against APOC3 called ARO-APOC3.

Similar to APOC3, the inactivation of ANGPTL3 using monoclonal antibodies (Evinacumab) (2-6), antisense oligonucleotides (ASOs) (Vupanorsen) (7, 8), and RNAi (ARO-ANG3) has been shown to significantly lower plasma LDL-C and TG levels in various dyslipidemic patients groups (9). Evinacumab was approved in 2021 as a treatment for homozygous familial hypercholesterolemia (HoFH), while Vupanorsen was discontinued in 2021 due to the limited reduction in non-HDL-C and TG and increases in liver fat and enzymes (10). Recent case reports suggest that Evinacumab may promote the regression of atherosclerotic plaques in HoFH patients (11, 12).

Whereas the clinical development of anti-APOC3 and -ANGPTL3 treatments have progressed well, therapies targeting ANGPTL4 have faced delay because mice deficient in ANGPTL4 develop lethal mesenteric lymphadenopathy and chylous ascites when fed a diet high in saturated fatty acids (13-15). Whether whole-body inactivation of ANGPTL4 might trigger similar pathological features in humans is unclear. As an alternative pharmacological strategy, inactivating ANGPTL4 specifically in the liver holds considerable promise (16).

Human genetic data can be leveraged to predict the clinical effect of the pharmacological inactivation of genes or proteins. Here, we aimed to compare the predicted therapeutic effects of APOC3, ANGPTL3, and ANGPTL4 inactivation by investigating the biological and clinical impact of inactivation variants in the respective genes. In addition, to address safety concerns, we compared the predicted detrimental effects of APOC3, ANGPTL3, and ANGPTL4 inactivation on relevant disease outcomes. We conclude that therapies specifically aimed at decreasing plasma ANGPTL3, ANGPTL4, and APOC3 levels are expected to reduce the risk of coronary artery disease without raising safety concerns. Therapies targeting ANGPTL4 levels are expected to favorably impact the risk of type 2 diabetes. This suggests that reducing ANGPTL4 could offer therapeutic advantages to a wider group of patients with dyslipidemia and type 2 diabetes.

87 **METHODS**

88 **Study design and data sources**

89 To estimate the causal effects of pharmacologically inactivating the *ANGPTL3*, *ANGPTL4*, and *APOC3*
90 genes, we performed two-sample drug-target Mendelian randomization analyses (MR). We used, as
91 instrumental variables (IV), genetic variants within 2.5 kilobase pairs (Kb) of the target gene that had
92 genome-wide significant associations (P-value $\leq 5\times10^{-8}$) with protein abundance and plasma TG, as
93 determined by genome-wide association studies (GWAS). Plasma protein abundance was measured in
94 GWAS using the SomaScan and Olink platforms (17, 18). GWAS data on plasma TG, LDL cholesterol,
95 HDL cholesterol, apolipoprotein B, apolipoprotein A1, and lipoprotein(a) were retrieved from the 2018
96 Neale Lab UK biobank analysis (http://www.nealelab.is/uk-biobank/). For the functional variant
97 analyses, genetic association data on TG, LDL cholesterol, and HDL cholesterol were retrieved from
98 the AstraZeneca UK biobank exome sequencing-based phenome-wide association study (PheWAS)
99 portal (19). We obtained outcome summary data from GWAS of six cardiometabolic disease endpoints,
100 16 cardiometabolic risk markers, 43 routine clinical chemistry tests, 11 internal organ MRI
101 measurements, and five abdominal lymphadenopathy-related phenotypes (see **Table 1**, **Supplemental**
102 **Table 1,** and **Supplemental Methods**). Phenome-wide MR analyses were conducted in FinnGen and
103 the UK biobank. FinnGen integrates genotype data from Finnish biobanks with longitudinal health
104 registry data (20). The UK Biobank is a large-scale research resource containing genetic, blood
105 chemistry, imaging, and health record data from half a million UK participants (21). FinnGen data freeze
106 10 and UK biobank meta-analysis (https://public-metaresults-fg-ukbb.finngen.fi) stores genetic
107 association statistics on 694 disease-related outcomes from 301,552–882,347 individuals. Further details
108 on the study design are given in the **Supplemental Methods**.

Table 1. Description of GWAS data sets

	Trait	First author (year)	Consortium	Sample size (events/total)	Population
pQTL	Plasma protein abundance (SomaScan)	Ferkingstad (2021) (17)	deCODE	35,559	Icelandic
	Plasma protein abundance (Olink)	Dhindsa (2023) (18)	Not available	50,829	British
Diseases	Coronary artery disease	Aragam (2022) (22)	CARDioGRAMplus C4D; EPIC-CVD	181,522 / 1,165,690	European
	Chronic kidney disease	Wuttke (2019) (23)	CKDGen	41,395 / 480,698	European
	Ischemic stroke	Mishra (2022) (24)	GIGASTROKE	62,100 / 1,296,908	European
	Non-alcoholic fatty liver disease	Ghodsian (2021) (25)	Not available	8,434 / 787,048	European
	Type 2 diabetes; Type 2 diabetes adjusted for Body Mass Index (BMI)	Mahajan (2018) (26)	DIAGRAM	74,124 / 898,130	European
Risk factors	Plasma total, HDL, and LDL cholesterol; Apolipoprotein B; Apolipoprotein A1; TG; Lipoprotein(a); HbA1c	Neale lab (2018)	Not available	273,896 – 344,278;	British
	HDL, and LDL cholesterol; TG; NMR metabolomics	Wang (2021) (19); Nag (2023) (27)	AZPheWAS	95,077 – 376,311	British
	NMR metabolomics, including total lipoprotein phospholipids	Elsworth (2020) (30)	MRC-IEU	110,058 – 115,078	British
	Systolic blood pressure; diastolic blood pressure	Evangelou (2018) (28)	Not available	757,601	European
	BMI; waist-hip ratio (with and without adjustment for BMI)	Pulit (2018) (29)	GIANT	694,649 – 806,834	European
	Body fat percentage; NMR total triglycerides; NMR total phospholipids	Elsworth (2020) (30)	MRC-IEU	115,078 – 454,633	British
	Plasma creatinine estimated glomerular filtration rate (eGFR); cystatin C eGFR	Stanzick (2021) (31)	CKDGen	1,004,040; 1,201,909	European; 86% European
Safety-related	Magnetic resonance imaging of internal organs	Liu (2021) (32)	Not available	25,617 – 32,860	British
	Routine blood chemistry tests	Neale lab (2018)	Not available	30,565 – 350,812	British
	Acute lymphadenitis; Acute peritonitis; Ascites; Intestinal malabsorption; Non-infectious lymphatic disorders	Neale lab (2018); Kurki (2023) (20)	Not available; FinnGen	620 – 4,982 / 270,172 – 382,633; 798 – 1643 / 295,812 – 341,350	British; Finnish
	Phenome-wide association study	FinnGen (2023) (20)	Pan-UK Biobank + FinnGen meta-analysis	110 – 279,543 / 301,552 – 882,347	British; Finnish

'NMR' indicates nuclear magnetic resonance spectroscopy.

Statistical methods

Drug-target MR analyses

In the drug-target MR analyses, we identified variants within 2.5 Kb of each gene associated (P-value ≤ 5×10^{-8}) with either plasma protein abundance (called *cis* protein quantitative trait loci, *cis*-pQTLs), or plasma TGs. The precision of the inverse-variance weighted (IVW) estimator can be influenced by LD-related correlation between the genetic IV in the drug target genes *cis'* position. Therefore, we used a generalized least squares (GLS) IVW MR estimator to correct for this potential source of bias (33, 34). The GLS-corrected MR approach can be conceptualized as combining the independent information of variants in the vicinity of a target gene while maintaining robust standard errors through weighting for their LD-related correlation. Variants in each target gene were clumped at an LD threshold of $r^2 \geq 0.10$ to avoid GLS-related multicollinearity issues. Further information regarding the methodology can be found in the **Supplemental Methods**.

A list of the genetic instruments used for the MR is provided in **Table 2**. Due to the complex LD structure of the *APOA1-APOA5-APOC3* locus, we supplemented the original analyses with a second model of APOC3 lowering. In this model, APOC3 lowering was instrumented through the *APOC3 c.55+1G>A* splice donor loss variant. Furthermore, we used *LPL* and genome-wide TG-associated variants as positive controls. *LPL* was analyzed using drug-target MR. For the genome-wide TG-associated variant MR, we tested the causal effect of TG using variants in chromosomes 1-22 associated with TG at P-value ≤ 5×10^{-8}. An LD clumping window of 500 Kb and a threshold of $r^2 \geq 0.001$ was applied before analysis using an IVW MR estimator.

Table 2. Genetic instruments

	rsID	Variant	HGVS	Consequence	Frequency	Effect (P-value) Protein	TG
ANGPTL3	rs79151558	1:62595131:A>G		Upstream variant	0.028	-0.32 (8.1e-39)	-0.06 (5.4e-13)
	rs11207997*	1:62596235:C>T		Upstream variant	0.338	-0.22 (1.2e-144)*	-0.08 (2.7e-221)*
	rs17123728	1:62602628:G>A	c.931+248G>A	Intron variant	0.04	n.s.	0.03 (2.5e-08)
	rs35285100	1:62603486:T>C	c.932-483T>C	Intron variant	0.071	0.10 (2.3e-09)	n.s.
	rs10789117*	1:62606594:A>C		Downstream variant	0.354	-0.22 (1.7e-144)*	-0.08 (1.6e-221)*
	rs6678483*	1:62608771:C>A		Downstream variant	0.354	-0.22 (1.7e-144)*	-0.08 (2e-221)*
ANGPTL4	rs116843064	19:8364439:G>A	p.Glu40Lys	Missense variant	0.024	-0.32 (6.6e-35)	-0.21 (3.2e-127)
	rs149480839	19:8368237:C>T	c.548-982C>T	Intron variant	0.03	n.s.	-0.05 (2.6e-14)
	rs139469000	19:8376253:C>T		Downstream variant	0.28	n.s.	-0.02 (1.7e-09)
APOC3	rs2727788	11:116828247:C>A		Upstream variant	0.262	n.s.	-0.05 (7.3e-83)
	rs138326449	11:116830638:G>A	c.55+1G>A	Splice donor variant	0.002	-2.19 (3.2e-142)	-0.86 (3.4e-157)
	rs5141	11:116831407:T>C	c.179+511T>C	Intron variant	0.916	-0.17 (2.1e-38)	-0.19 (<2e-308)
	rs5132	11:116832062:C>T	c.180-702C>A	Intron variant	0.015	n.s.	0.06 (3.1e-08)
	rs12721031	11:116833789:C>T		Downstream variant	0.023	n.s.	-0.06 (2.6e-12)
	rs10750098	11:116834852:G>T		Downstream variant	0.115	-0.17 (2.1e-38)	-0.19 (<2e-308)
	rs12721028	11:116834874:A>G		Downstream variant	0.159	n.s.	0.04 (2e-35)
	rs12718462	11:116835003:T>C		Downstream variant	0.066	n.s.	-0.05 (1.8e-22)

Showing the genetic variants that were selected for inclusion as instrumental variables in one or more of the MR analyses whose results are shown in **Figures 1-3**. The specific instruments used in each separate MR analysis are provided in **Supplemental Table 2**. Variant consequences were retrieved from the Ensembl Variant Effect Predictor (version 109) (38). 'Effect' indicates the 1 s.d. protein abundance (retrieved from (17)) or mmol/L TG change (retrieved from http://www.nealelab.is/uk-biobank/) per allele. 'rsID' denotes Reference single nucleotide polymorphism ID. 'HGSV' indicates Human Genome Structural Variation Consortium nomenclature for sequence variants.

* These three variants were in strong linkage disequilibrium (LD) and, therefore, showed the same associations with TG levels and plasma ANGPTL3 abundance. Because they were in strong LD, they were never included in the same MR model (see **Supplemental Table 2**).

Sensitivity analyses

Drug-target MR substantially relies on the assumption that LD (a phenomenon in which neighboring genetic variants are inherited together more frequently than anticipated by chance (35)) does not confound the association between variant and outcome. In cases where there are distinct genetic variants affecting both the exposure and the outcome, and they are connected through LD, there is a risk of making incorrect conclusions (36). To limit this issue, we performed colocalization analyses, which test whether two independent association signals in the same gene region are consistent with having a single shared causal variant (that is, testing if the association signals are 'colocalized') (37). To assess possible confounding from LD, all drug target MR analyses were complemented by colocalization analysis of the 500 Kb (±250 Kb) region surrounding each target gene (37). Further details regarding colocalization, LD matrix sensitivity, and sample overlap bias analyses are provided in the **Supplemental Methods**.

We performed sensitivity MR analyses of *ANGPTL3*, *ANGPTL4*, *APOC3*, *LPL*, and *LIPG* on CAD, by restricting the genetic instrument selection to variants within these target genes that are predicted to have functional impacts. This strategy aimed to mitigate potential biases arising from common non-coding small-effect variants outside the target genes, which could be confounded due to linkage disequilibrium with other genes in the same genomic region. Ensembl Variant Effect Predictor (VEP) version 109 (38) was used to annotate the variants within 2.5 Kb of the gene that were associated ($P \leq 0.01$) with target protein levels and any plasma lipid measurement (ApoB, ApoA-I, TG, HDL-C, or LDL-C) in (19). Non-coding variants outside of the 5' untranslated region (UTR), 3' UTR, or splice site regions were filtered out and excluded from further analysis, as were missense variants lacking SIFT deleterious or PolyPhen likely or probably damaging annotations. MR was conducted for single variants using the Wald ratio estimator, and meta-analysis was performed using a random-effects IVW estimator.

Lymphadenopathy and phenome-wide MR analyses

A Wald ratio estimator was used for the single-variant MR of lymphadenopathy-related phenotypes and the phenome-wide MR conducted in FinnGen (39). The variants were selected based on being within 2.5 Kb of the drug target gene, their strength of association with target protein plasma abundance ($P \leq 5\times10^{-8}$), their strength of association with triglyceride levels ($P \leq 5\times10^{-8}$), and their functional consequence (the same criteria as outlined above for the CAD MR limited to functional variants).

Genetic mimicry analyses

Genetic mimicry analysis was used to compare the metabolic concordance of common and rare variants in the genes *ANGPTL3*, *ANGPTL4*, and *APOC3.* This method uses linear regression to determine the extent of similarity between different variants' genetic associations in high-dimensional data sets (40, 41). The degree of concordance is given as the coefficient of determination (R^2). Genetic association effect estimates for the common variants (CVs) were derived using drug-target MR with plasma TGs as the exposure. The PTV estimates were extracted from the *ptv5pcnt* collapsing models from the Astra

175 Zeneca PheWAS portal (27). Gene variant-metabolite association pairs with an association strength of
176 P ≥ 0.10 were excluded from the analyses. The collapsing model estimates were scaled by their 1-s.d.
177 effect on plasma TGs to improve interpretability.
178
179 **Meta-analysis of the impact of loss-of-function variants on CAD**
180 We conducted a meta-analysis to assess how loss-of-function (LoF) variants in *ANGPTL3*, *ANGPTL4*,
181 and *APOC3* impact the risk of CAD. To minimize the influence of incorrect genotype calls for rare
182 variants, the meta-analysis was limited to studies where genotypes were determined by DNA
183 sequencing. When multiple papers reported on individuals from overlapping cohorts or case-control
184 studies, we selected the substudy with the largest sample size for inclusion in the meta-analysis. We
185 determined the impact of the inactivating variants on CAD risk per mmol/L reduction of TG and per
186 inactivating allele using fixed-effect IVW estimators. If no within-sample association of inactivating
187 variants with TG concentrations (in mmol/L) was available, the combined IVW meta-analysis TG
188 estimate was used as the denominator to determine the CAD odds per mmol/L TG effect. UK biobank
189 LoF variants associated with CAD (UKB Phenotypic Release v51165: "union#I25#Chronic ischaemic
190 heart disease") were retrieved from the Astra Zeneca PheWAS portal using the *flexdmg*, *flexdmg,* and
191 *ptv5pcnt* models for *ANGPTL3*, *ANGPTL4*, and *APOC3*, respectively (19). Statistical heterogeneity
192 across studies was estimated by calculating the Cochran Q statistic.
193
194 **Multiple testing**
195 P-values and 95% confidence intervals (CI) are reported using analysis-type Bonferroni multiple
196 comparisons correction. In the primary MR analyses, we corrected for the six cardiometabolic disease
197 outcomes that were run across three different drug-target gene exposures (*ANGPTL3, ANGPTL4,*
198 *APOC3*) for protein abundance, and four genes for the TG exposure (*ANGPTL3, ANGPTL4, APOC3,*
199 *LPL*). Additionally, we included sixpolygenic MR models, totaling 48 multiple comparisons for the
200 cardiometabolic disease outcomes. In the cardiometabolic risk factor MR analyses of *cis*-pQTLs, we
201 made corrections for 48 multiple comparisons (16×3). Similarly, imaging and clinical chemistry MR
202 analyses were corrected for 33 (11×3), and 129 (43×3) multiple comparisons, respectively. We did not
203 perform multiple comparison corrections for the *ANGPTL4*-targeted MR analyses of the
204 lymphadenopathy-related phenotypes. This was because identifying potential safety concerns that
205 needed to be addressed was considered more critical than stringent multiplicity correction for these
206 specific outcomes. Similarly, the primary motivation for performing the functional variant-limited CAD
207 MR analyses and rare inactivating variant meta-analysis was to reduce the risk of false-negative
208 findings. Additionally, we wanted to ensure that these CIs and P-values remained comparable across
209 different studies. These CIs and P-values were, therefore, not corrected for multiple comparisons. The
210 significance threshold in the phenome-wide *cis*-pQTL MR analyses was set at 2082 multiple
211 comparisons (694 phenotypes in the FinnGen R10 and UK biobank meta-analysis, times three genes).

212 **RESULTS**

213 The results of the drug-target MR analyses of cardiometabolic diseases, cardiometabolic risk factors,
214 and the safety-related endpoints are presented in **Figure 1**, **Figure 2**, and **Figure 3**, respectively. MR
215 scatter, colocalization plots, and results tables with greater detail are provided in **Supplemental Figures**
216 **1-2** and **Supplemental Table 2**. Detailed PheWAS results are provided in **Supplemental Tables 6-9**.
217

218 **Drug-target MR of cardiometabolic diseases**

219 Genetically mediated changes in plasma ANGPTL3 protein abundance were not associated with a
220 reduced risk of any cardiometabolic outcome (**Figure 1A**). Neither were *ANGPTL3*-mediated changes
221 in plasma TG (**Figure 1B**). The p.E40K coding variant was the only variant that qualified as a *cis*-pQTL
222 in the *ANGPTL4* region. *ANGPTL4* p.E40K is a common missense variant (allele freq. ~2% in
223 Europeans) that destabilizes ANGPTL4 after secretion and prevents ANGPTL4 from inhibiting LPL
224 (42). Changes in ANGPTL4 protein abundance via *ANGPTL4* p.E40K were associated with a decreased
225 risk of CAD (OR: 0.57, $P=2\times10^{-19}$), T2D (OR: 0.73, P=0.002), and T2D adjusted for BMI (OR: 0.61,
226 $P=2\times10^{-7}$) (**Figure 1A**). Similarly, changes in plasma TG levels via three *ANGPTL4* variants were
227 associated with a decreased risk of CAD (OR: 0.43, $P=2\times10^{-21}$), T2D (OR: 0.62, $P=7\times10^{-4}$), and T2D
228 adjusted for BMI (OR: 0.47, $P=4\times10^{-8}$) (**Figure 1B**). In addition, colocalization analyses indicated a
229 high probability of *ANGPTL4* p.E40K being a shared causal variant for ANGPTL4 abundance and TG
230 levels with CAD, T2D, and T2D adjusted for BMI, respectively (pp. H_4: 98–100%) (**Figures 1A-B**).
231 Changes in APOC3 levels caused by *APOC3* variants were associated with a reduced risk of CAD (OR:
232 0.90, P=0.014) (**Figure 1A**), as were changes in TG levels through *APOC3* variants (OR: 0.80, $P=6\times10^{-}$
233 ^{11}). The *APOC3* c.55+1G>A splice donor loss variant had a substantial impact on plasma APOC3 levels
234 (-2.19 s.d. protein, $P=3.2\times10^{-142}$) (**Table 2**). When compared to the model allowing for multiple variants
235 in the *APOC3* region, APOC3 lowering modeled through the *APOC3* c.55+1G>A variant demonstrated
236 a comparable correlation with CAD in terms of the direction of its effect. However, the association was
237 non-significant (**Figure 1**).

238 Similar to APOC3 and ANGPTL4, changes in plasma TG levels through *LPL* variants were associated
239 with a reduced risk of CAD (OR: 0.69, $P=2\times10^{-24}$), NAFLD (OR: 0.66, P=0.03), and T2D (OR: 0.80,
240 $P=6\times10^{-11}$) (**Figure 1B**).
241

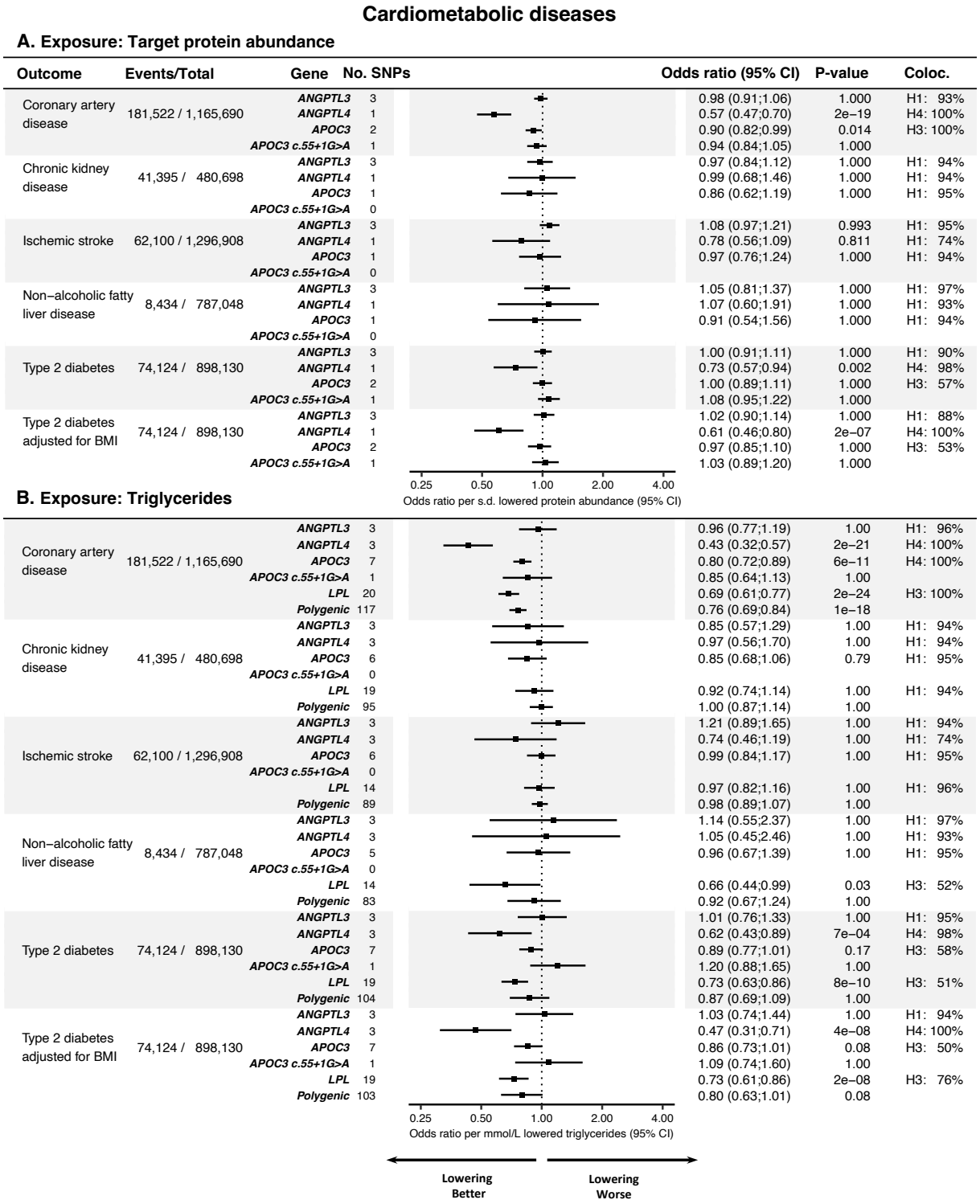

Figure 1. Results of MR analyses of cardiometabolic disease outcomes.

A: Forest plot and table of the *cis*-pQTL-based MR analyses. 'Events/total' indicates the outcome study's case count and total sample size. 'No. SNPS' specifies the number of variants included in the MR model. Zero SNPs indicate that none of the genetic instruments were detected in the outcome data set. 'Coloc.' shows the colocalization hypothesis ($H_{0\text{-}4}$) with the highest posterior probability (see the 'Methods' section for details about their interpretation). **B:** Results of the MR analysis using TG levels as the exposure.

Drug-target *cis*-pQTL MR of cardiometabolic risk factors

Genetically lowered plasma ANGPTL3 levels mediated through *ANGPTL3* variants were associated with reduced total cholesterol (-0.27 mmol/L, $P=2\times10^{-107}$), TG (-0.34 mmol/L, $P=6\times10^{-206}$), LDL-C (-0.15 mmol/L, $P=2\times10^{-57}$), ApoB (-0.03 g/, $P=3\times10^{-36}$), and ApoA-I levels (-0.05 g/L, $P=1\times10^{-51}$), while the effect on HDL-C was comparatively weak (-0.02 mmol/L, $P=4\times10^{-5}$) (**Figure 2**).

Genetically lowered plasma ANGPTL4 levels instrumented through the p.E40K variant were associated with reduced plasma TG (-0.65 mmol/L, $P=1\times10^{-125}$) and weakly reduced ApoB levels (-0.02 g/L, P=0.04), as well as increased ApoA1 (0.11 g/L, $P=2\times10^{-55}$) and HDL-C levels (0.24 mmol/L, $P=8\times10^{-134}$) (**Figure 2**). Genetically lowered plasma ANGPTL4 levels were also associated with modest reductions in the waist-hip ratio (-0.09 s.d., P=0.005), and the waist-hip ratio adjusted for BMI (-0.12 s.d., $P=2\times10^{-5}$), and a small increase in body fat percentage (0.07 s.d., P=0.009) (**Figure 2**).

Genetically lowered plasma APOC3 levels were associated with reduced TG levels (-0.58 mmol/L, $P < 2\times10^{-308}$) (**Figure 2**). APOC3 levels were also associated with ApoB (-0.03 g/L, $P=3\times10^{-22}$), LDL-C (-0.10 mmol/L, $P=7\times10^{-18}$), HDL-C (0.16 mmol/L, $P < 2\times10^{-238}$), and total cholesterol (-0.08 mmol/L, $P=5\times10^{-6}$) (**Figure 2**). In terms of association and effect directionality, these results closely resembled those of the *APOC3 c.55+1G>A* model (**Figure 2**).

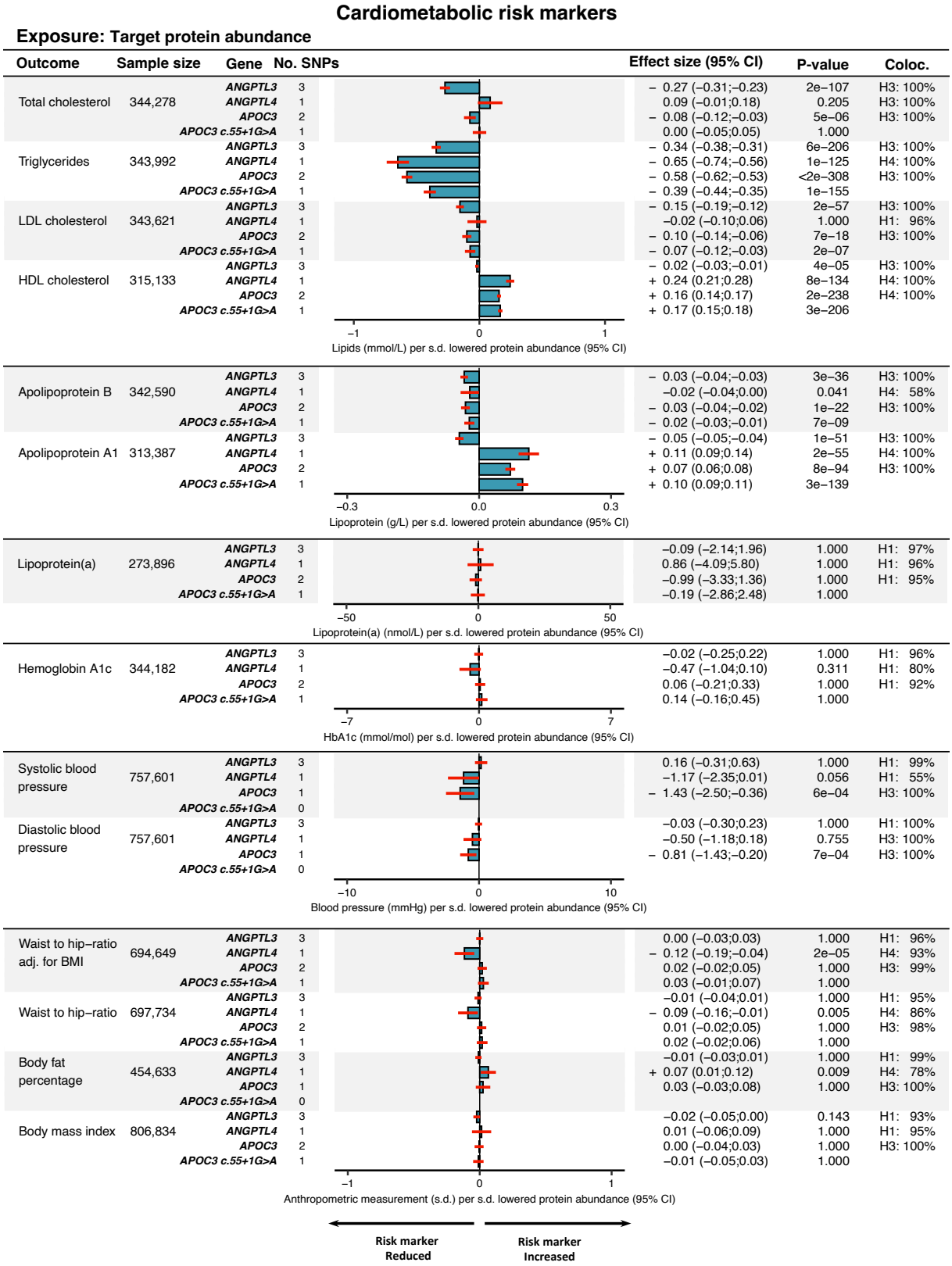

Figure 2. Results of MR analyses of cardiometabolic disease risk factors.
The results are presented as bar plots, showing the magnitude of the effect per s.d. lowered protein abundance. The red lines indicate the 95 % CI. The results from cis-pQTL MR of the estimated glomerular filtration rate (eGFR) by Cystatin C and plasma Creatinine, respectively, are given in **Supplemental Figure 3**.

Drug-target MR of potential adverse effects

Genetic lowering of plasma protein levels of the target genes was not associated with any of the MRI imaging endpoints (**Figure 3A**). 9, 3, 9, and 6 out of the 43 routine clinical laboratory tests showed statistically significant associations by drug-target cis-pQTL MR of the *ANGPTL3*, *ANGPTL4*, *APOC3,* and *c.55+1G>A* models, respectively (**Figure 3B**). The effect magnitudes were weak. For example, genetically lowered ANGPTL3 and APOC3 levels were significantly associated with increased platelet count. However, the effect was estimated to be 4–5×10^9 cells/L per s.d. lowered plasma protein levels, which was minimal compared to the population mean value of 252×10^9 cells/L.

Given that safety concerns have arisen from preclinical models of ANGPTL4 deficiency, we conducted targeted cis-pQTL MR analyses of *ANGPTL4* on disease phenotypes that may be associated with abdominal lymphadenopathy. The mechanism behind the fatal chylous lymphadenopathy observed in mice was purportedly the loss of inhibition of LPL in macrophages, which caused them to take up excess lipids, leading to massive inflammation in the mesenteric lymph system (14). Exposure to *ANGPTL4* suppression was instrumented using two different models: by the ANGPTL4 p.E40K coding variant, and by the ANGPTL4 p.Cys80frameshift (fs) variant. *ANGPTL4* p.Cys80fs is a high-confidence predicted LoF variant. It is enriched in Finns compared to non-Finnish Europeans (allele frequency: 0.63% vs. 0.05%). *Cis*-pQTL MR via the relatively common *ANGPTL4* p.E40K variant was conducted at five different phenotypes that may be related to lymphadenopathy and malabsorptive states. Four had overlapping phenotype codes between the UK biobank and FinnGen and were meta-analyzed using IVW meta-analysis. ANGPTL4 levels via p.E40K were not associated with any of the five phenotypes (**Figure 3C**). However, since the confidence intervals were wide, we cannot fully exclude an association of p.E40K within this interval. Genetically lowered plasma ANGPTL4 levels via the *ANGPTL4* p.Cys80fs variant were not associated with any of the four FinnGen phenotypes that may be related to lymphadenopathy and malabsorptive states (**Figure 3C**).

To investigate if there was any genetic evidence for unknown ANGPTL4-mediated side effects, we performed cis-pQTL MR on 694 disease-related phenotypes in FinnGen and the UK Biobank via the *ANGPTL4* p.E40K and p.Cys80fs variants. Using a phenome-wide significance threshold of $P \leq \frac{0.05}{3\times694}$, we found no evidence for increased risk of any endpoint via p.E40K- or p.Cys80fs-lowered ANGPTL4 levels (**Figure 3D**). Instead, we found phenome-wide evidence that p.E40K reduced the risk of four CAD-related phenotypes, including myocardial infarction and one T2D-related phenotype, while also being associated with a lowered probability of statin prescription, lipoprotein disorders, and hypercholesterolemia (**Figure 3D**). Additionally, *ANGPTL4* p.Cys80fs was associated with a decreased risk of two T2D-related outcomes and a lowered probability of statin prescription and hypercholesterolemia diagnosis (**Figure 3D**).

The phenome-wide MR results of lowered plasma ANGPTL4 levels were compared with ANGPTL3 and APOC3 by cis-pQTL MR of the 694 FinnGen and UK Biobank endpoints using the *ANGPTL3*

306 c.*52_*60del and *APOC3* c.55+1G>A. Genetically lowered plasma ANGPTL3 levels were associated
307 with a reduced risk of being prescribed statin medication, two lipid-related diagnosis codes but not any
308 other patient-related outcome (**Supplemental Figure 3A**). *APOC3 c.55+1G>A* was associated with a
309 reduced risk of statin prescription but not any other endpoint (**Supplemental Figure 3B**).

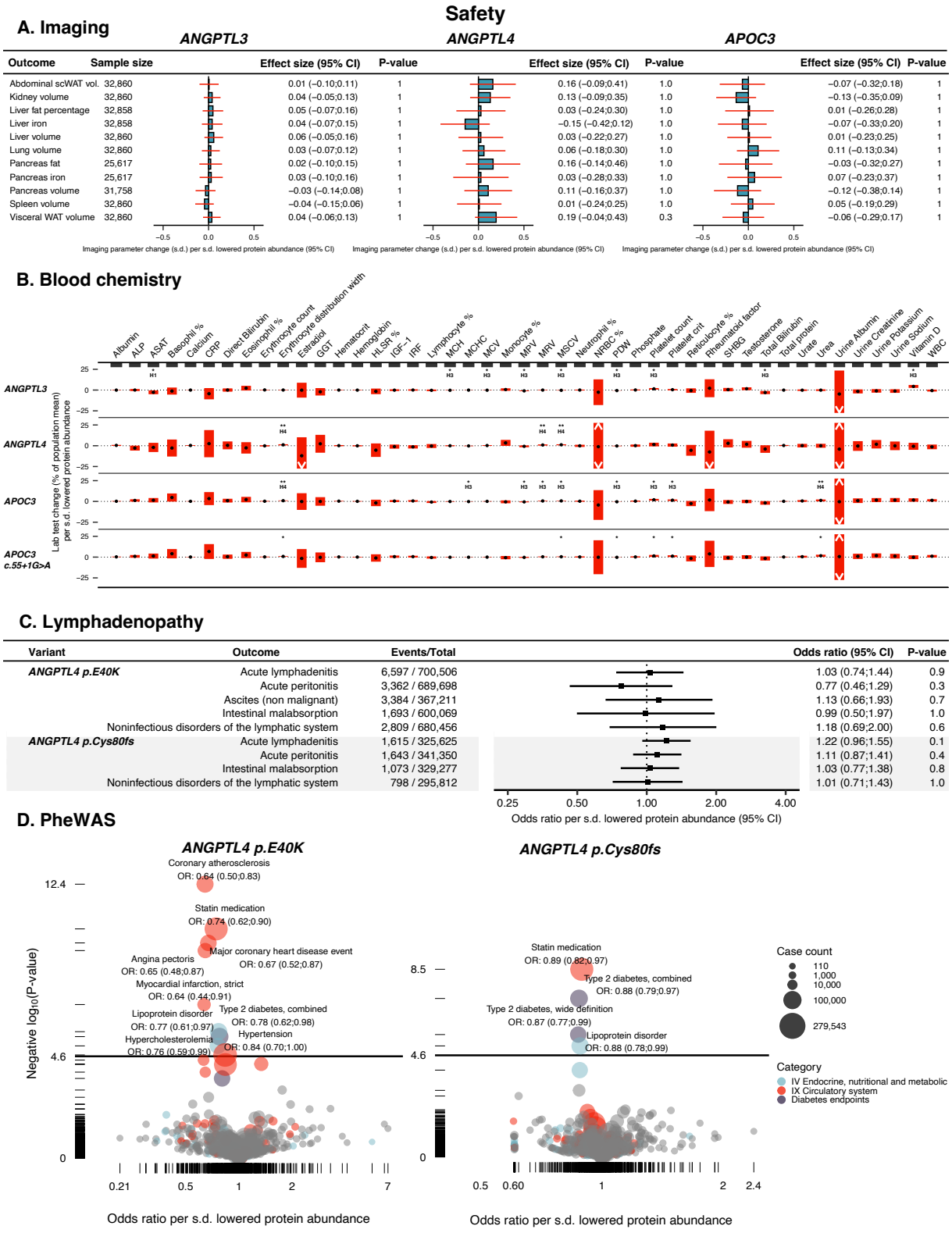

Figure 3. Results of MR analysis of potential adverse effects.
A: *Cis*-pQTL MR results on the imaging outcomes. Bar plots and red lines indicate the effect and 95% CI:s. 'scWAT' indicates subcutaneous white adipose tissue. 'vol.' indicates volume. **B:** *Cis*-pQTL MR of the clinical laboratory outcomes. The red bars indicate the 95 % CI. The black dots indicate the effect point estimate. '*' indicate $P < 0.05$. '**' indicates $P < 0.05$ with a shared causal variant (H_4). A list explaining the abbreviations is provided in the supplemental material (**Table S1**). **C:** Results of ANGPTL4 *cis*-pQTL MR of mesenteric lymphadenopathy and malabsorption-related phenotypes. **D:** Volcano diagram displaying the results of ANGPTL4 *cis*-pQTL phenome-wide MR scans on 694 outcomes in the FinnGen and UK Biobank meta-analysis. The *y*-axis solid straight lines indicate the phenome-wide significance threshold.

Common variants in *ANGPTL3*, *ANGPTL4*, and *APOC3* share their metabolic fingerprint with loss-of-function variants

In line with a previous investigation (43), we found no significant association between *ANGPTL3* suppression via common variants and CAD. Previously, however, evidence was presented that loss-of-function variants in *ANGPTL3* are associated with a decreased risk of CAD (44, 45). As the common variants in *ANGPTL3* presented here only modestly impacted plasma lipids, it could be argued that they do not accurately reflect the effects of more profound *ANGPTL3* suppression. Therefore, we examined whether common variants in *ANGPTL3*, *ANGPTL4*, and *APOC3* mimicked the effects (that is, showed the same effect directionality) of more deleterious protein-truncating variants (PTVs). PTVs often result in protein loss-of-function and, accordingly, are powerful genetic instruments to study the potential impact of pharmacological gene silencing (46).

All common variants in *ANGPTL3*, *ANGPTL4*, and *APOC3* were highly concordant with PTVs within the same gene (**Figure 4A-C**). One hundred thirty-seven metabolite associations in *ANGPTL3* showed a high concordance metric (R^2) of 85% between the common variants and PTV models. *ANGPTL4* common variants were also highly concordant with *ANGPTL4* PTVs, having an R^2 of 89% for a set of 86 metabolites, while *APOC3* showed a concordance metric R^2 of 91% in 137 metabolic parameters. These results demonstrate that the common genetic variations in *ANGPTL3*, *ANGPTL4,* and *APOC3* would be valid genetic instruments reflecting a modest "knock-down" of each respective gene.

Comparative drug-target MR of LPL and endothelial lipase (EL) reveals that in order to achieve CAD benefits, ANGPTL3 inhibition should primarily target LPL rather than EL

ANGPTL3 targets both EL and LPL and may thus influence CAD via two independent pathways (47). To compare the effects of these two target enzymes, we analyzed the effects of genetically instrumented EL and LPL activity on CAD by performing functional-variant limited MR of the *LIPG* (encoding EL) and *LPL* genes. We used the preferred enzyme substrate as the exposure, using plasma lipoprotein phospholipids for EL and total plasma TGs for LPL. We detected two functional *LPL* variants and four functional *LIPG* variants that had small to large effects on plasma TG/lipoprotein phospholipids (range: 0.02 – 0.6 s.d. per allele). Allele frequencies and imputation quality ('INFO' score) are given in **Figure 4D**.

MR analysis of *LPL* and *LIPG* found opposing significant associations for LPL (IVW meta-analysis: OR: 0.74, $P=1\times10^{-4}$) and EL (IVW meta-analysis OR: 1.38, $P=5\times10^{-7}$) (**Figure 4D**). These findings suggest that increased activity of LPL protects against the development of atherosclerosis, whereas heightened activity of EL may contribute to the acceleration of atherosclerosis. The contrasting impact of genetic EL and LPL activity on the risk of CAD suggests that in order to provide any net decrease in CAD risk, *ANGPTL3* inactivation may have to profoundly impact LPL activity more than EL activity.

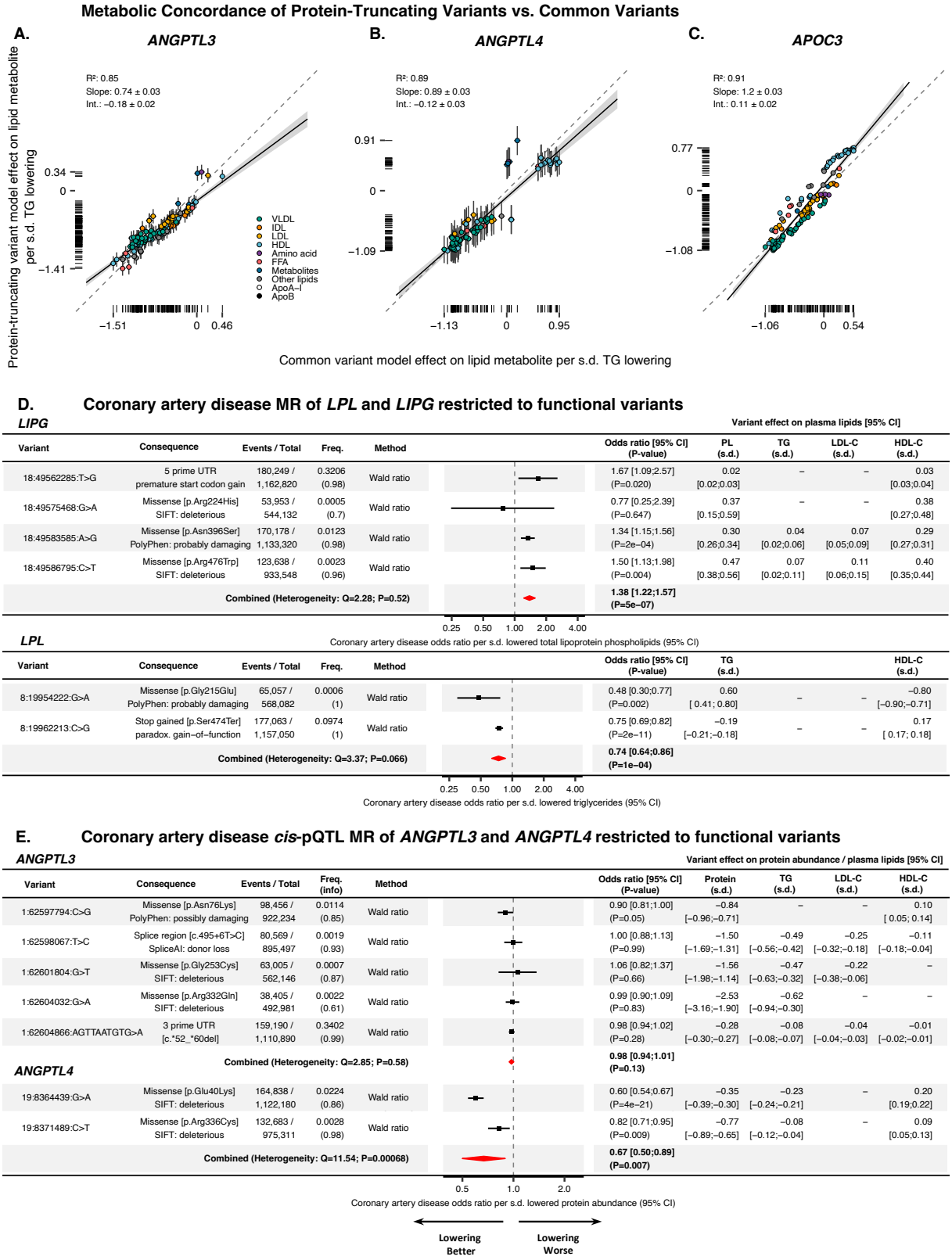

Figure 4. Results of sensitivity analyses.
The concordance between the effect directionality of CVs and PTVs is displayed using scatter plots with a regression line. **A:** Comparison of the effect directionality between *ANGPTL3* CVs and PTVs. **B:** *ANGPTL4* CVs vs. PTVs. **C:** *APOC3* CVs vs. PTVs. 'R²' represents the coefficient of determination. 'Int.' indicates the regression line intercept. The color of the scattered dots indicates the lipid class of the NMR parameter. **D:** Forest plots and tables showing the results of the CAD MR analysis focusing on functional variants in *LPL* and *LIPG*. Genetic association summary statistics of *LIPG* with the exposure were extracted from the UK biobank NMR study of 115,078 individuals retrieved from (30). *LPL* variant associations were retrieved from the same data set. CAD data was from the Aragam et al. meta-analysis (22). **E:** Forest plots and tables showing the results of the CAD

363 MR analysis that limited the selection of genetic instruments to functional variants in *ANGPTL3* and *ANGPTL4*. "Freq."
364 represents the frequency of the alternative allele. "info" represents the imputation quality metric derived from the outcome
365 GWAS. Variant effects on plasma lipids were retrieved from (19). The *ANGPTL4* p.Glu40Lys (p.E40K) estimates differ slightly
366 from *Figure 1* because the plasma protein abundance was determined using a different method (Olink (18), instead of
367 SomaScan (17)). There was significant heterogeneity for the ANGPTL4 IVW estimate (Cochran's Q: 11.54, P-value: 0.00068),
368 which likely was a consequence of the *ANGPTL4* p.Arg336Cys coding variant disproportionally affecting TG levels, compared to
369 the *ANGPTL4* p.E40K coding variant. This was supported by the fact that CAD MR by *ANGPTL4* variants using TG levels as the
370 exposure found no significant heterogeneity (Cochran's Q: 2.3, P-value: 0.13) (**Supplemental Figure 5**).

371 **Loss-of-function variants in *ANGPTL3*, *ANGPTL4*, and *APOC3*, and the risk of CAD**
372 Two previous exome-sequencing studies found LoF variants in *ANGPTL3* to be protective of CAD (3,
373 44). In an effort to reproduce these findings, we performed a sensitivity MR analysis of CAD and limited
374 the selection of genetic instruments to functional variants. Functional annotations were detected for five
375 *ANGPTL3*, two *ANGPTL4*, and one *APOC3* variant. The detected *APOC3* variant was the *c.55+1G>A*
376 splice donor loss variant, which was already reported in **Figures 1-3**. The other variants lowered protein
377 abundance, with impact sizes ranging from profound to modest (range: -2.53– -0.28) (**Figure 4E**) (18).
378 The variants were analyzed individually and together using random-effects IVW meta-analysis. *Cis*-
379 pQTL MR of the *ANGPTL3* variants indicated that ANGPTL3 protein levels were not significantly
380 associated with CAD, either individuallyor together (meta-analysis IVW OR: 0.98, P=0.13) (**Figure**
381 **4E**). By contrast, reduced *ANGPTL4* protein levels were associated with a decreased risk of CAD (meta-
382 analysis IVW OR: 0.67, P=0.007) (**Figure 4E**).
383 Considering the beneficial effects of ANGPTL3, ANGPTL4, and APOC3 on plasma lipids, it was
384 expected that genetic inactivation of these genes would confer protection against CAD. However, the
385 MR analyses focusing on common variants of *ANGPTL3*, as well as MR of functional variants (both
386 rare and common, identified through DNA microarray technology), did not support this hypothesis.
387 Therefore, we pursued a meta-analysis of DNA sequencing-based studies that studied the effect of
388 *ANGPTL3*, *ANGPTL4*, and *APOC3* LoF variants on CAD. The rationale for excluding DNA microarray
389 and exome bead chip-based studies was that they could potentially introduce measurement error for rare
390 variants (48, 49). This would lead to bias towards the null hypothesis. DNA-sequencing-based
391 substudies from previous papers (3, 44, 50, 51), were extracted and analyzed together with the chronic
392 ischemic heart disease case-control subset in the UK biobank (19). The total number of individuals
393 included in the meta-analysis amounted to 372,837 for *ANGPTL3*, 189,672 for *ANGPTL4*, and 160,230
394 for *APOC3*. The carrier status of LoF variants was associated with substantial decreases in protein levels
395 for both *ANGPTL3* (-1.73 s.d. protein, $P=3.2\times10^{-121}$) and *ANGPTL4* (-1.65 s.d. protein, $P=1.5\times10^{-102}$).
396 APOC3 protein levels were not measured in the UK Biobank. However, *APOC3* LoF variants were
397 associated with a significant reduction in TG levels (**Figure 5**).
398 The results of the meta-analysis are presented in **Figure 5**. The presence of *ANGPTL3* LoF variants
399 was associated with reduced CAD risk (meta-analysis IVW OR: 0.45 per TG, $P=5.3\times10^{-7}$). *ANGPTL4*
400 LoF variant carrier status, excluding p.E40K, was also associated with a reduced risk of CAD (meta-
401 analysis IVW OR: 0.35 per TG, P=0.017), as was *APOC3* LoF variant carriers status (meta-analysis
402 IVW OR: 0.80 per TG, P=0.021). The key finding was the robust association of *ANGPTL3* LoF carrier
403 status with a reduced risk of CAD. This association was not detected by the other approaches and
404 implies that ANGPTL3 lowering might offer similar atheroprotective benefits comparable to those
405 achieved by ANGPTL4 or APOC3 lowering.

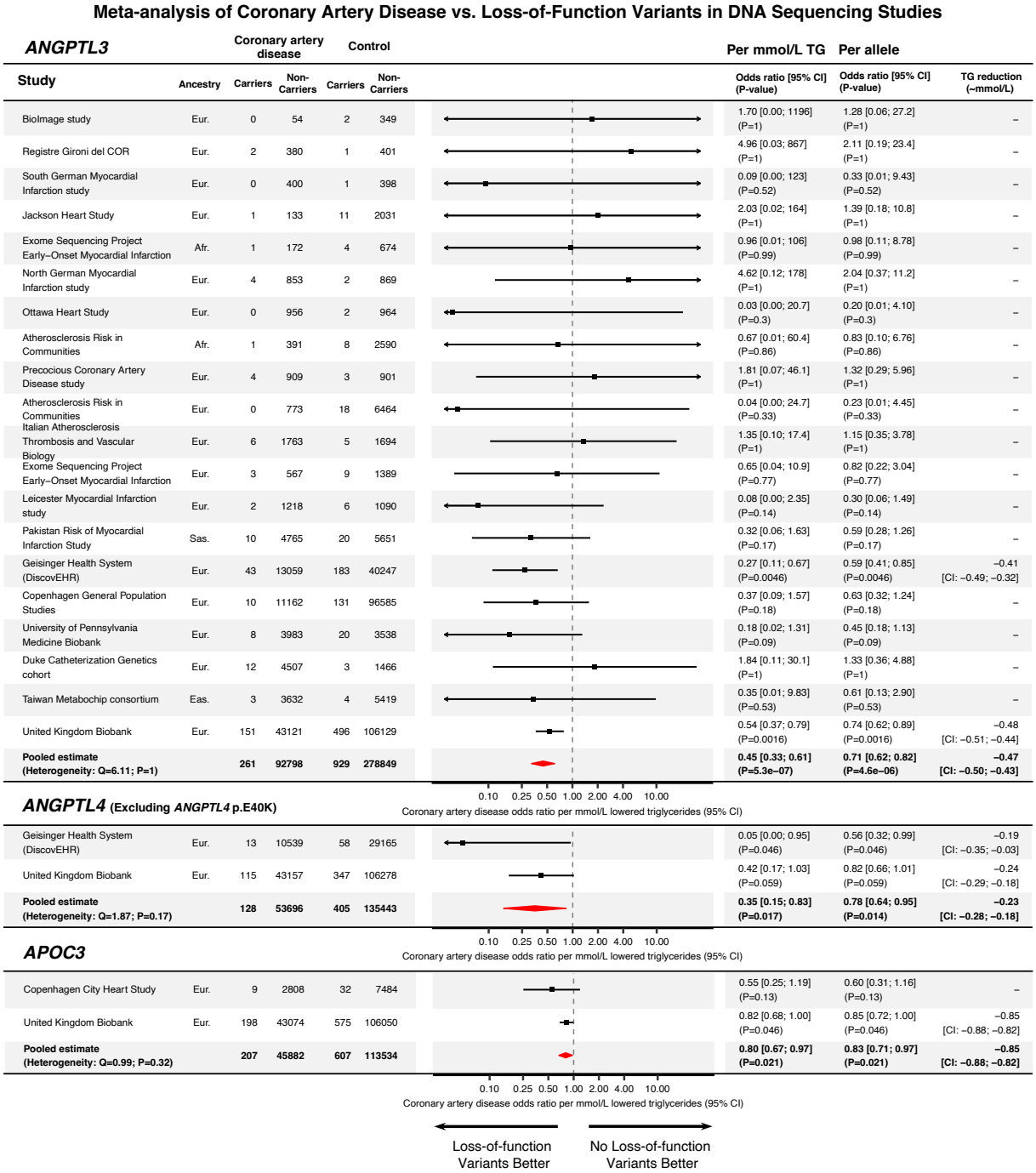

Figure 5. Meta-analysis of loss-of-function variants in ANGPTL3, ANGPTL4, and APOC3, and the risk of CAD. Forest plots and tables indicating the effect on CAD per TG, and per allele. The loss-of-function variant effect estimates for each substudy were retrieved from (3, 19, 44, 50, 51). The case definition used in the Copenhagen City Heart Study was not exclusively restricted to CAD. 21% of the ischemic vascular disease cases were diagnosed with atherosclerotic cerebrovascular disease, rather than CAD, which encompassed 79 % of the cases (51). ‘Afr.’ indicates African ancestry. 'Eas.' indicates East Asian ancestry. ‘Eur.’ denotes European ancestry. 'Sas.' denotes South Asian ancestry.

413 **DISCUSSION**

414 We find that targeted inactivation and associated lowering of plasma APOC3 levels is predicted to
415 decrease plasma TG and LDL and raise HDL levels. Targeted lowering of plasma ANGPTL3 is expected
416 to reduce plasma TG, LDL, and HDL levels, while lowering of plasma ANGPTL4 is predicted to
417 decrease plasma TG and increase HDL levels. Based on these findings, it is expected that genetic
418 inactivation of APOC3, ANGPTL3, and ANGPTL4 levels is associated with protection against CAD.
419 Through MR and a meta-analysis of rare variant genetic association studies, we confirmed that targeted
420 inactivation and lowering of ANGPTL3, ANGPTL4, and APOC3 is associated with a lowered risk of
421 CAD. In addition, lifetime genetic lowering of ANGPTL4 was observed to reduce the risk of T2D,
422 indicating that ANGPTL4 inhibition might provide additional benefits to patients with T2D and
423 dyslipidemia.

424 The inactivation of ANGPTL4 in mice and monkeys was shown to lead to mesenteric lymphadenopathy
425 and other severe complications. Naturally, these observations raised serious concerns about the safety
426 of pharmacological targeting of ANGPTL4. Here, we did not find an association between genetic
427 ANGPTL4 inactivation and several disease codes related to lymphatic disorders. While these data do
428 not entirely exclude any harmful effects of ANGPTL4 inactivation, they do mitigate safety concerns
429 about the impact of whole-body inactivation of ANGPTL4 in humans. Recently, it was shown that
430 silencing of ANGPTL4 in the liver and adipose tissue using ASO markedly reduces plasma TG levels
431 in mice yet does not lead to mesenteric lymphadenopathy or other complications (16). These data
432 suggest that liver- and adipose tissue-specific inactivation of ANGPTL4 may confer similar
433 cardiovascular benefits as whole-body ANGPTL4 inactivation without any particular safety risks.

434 Previous studies reported conflicting findings regarding the association between ANGPTL3 and CAD.
435 Dewey et al. (3), and Stitziel et al. (44) found that rare LoF *ANGPTL3* variants were associated with
436 decreased odds of ASCVD, whereas MR studies of common ANGPTL3-lowering variants reported
437 negative findings (43). By meta-analysis of rare LoF variant genetic association studies, we found clear,
438 statistically robust evidence that lifetime genetic inactivation of ANGPTL3 confers protection against
439 CAD. These findings are in line with recent case reports indicating that ANGPTL3 lowering with
440 Evinacumab protects against atherosclerosis progression in HoFH patients (11, 12).

441 The discrepancy between the rare LoF and common variant studies of ANGPTL3's association with
442 CAD could be due to a range of different factors. One possible explanation is the pleiotropic effects of
443 ANGPTL3. Besides inhibiting LPL, ANGPTL3 inhibits endothelial lipase (EL) (52). In a recent paper,
444 we showed that the LPL-independent effects of ANGPTL3 inactivation on plasma metabolic parameters
445 showed a striking inverse resemblance with EL inactivation, suggesting that ANGPTL3 modulates
446 plasma lipid levels by inhibiting LPL and EL (40). Here, using MR, we compared the effects of
447 genetically instrumented EL and LPL activity on CAD. Whereas increased LPL activity reduced the
448 odds of CAD, increased EL activity increased the odds of CAD. The observed link between EL and
449 CAD is consistent with previous human genetic studies showing the possible harmful effects of a

genetically predicted increase in EL activity (53, 54). This suggests that ANGPTL3's interaction with EL might counteract its cardiovascular benefits achieved through LPL inhibition under certain physiological conditions. While our research demonstrated metabolic concordance between ANGPTL3 common variants and LoF variants, it remains possible that more profound ANGPTL3 inactivation by LoF variants could tip the balance in favor of LPL inhibition over EL. This shift could potentially enhance the anti-atherosclerotic benefits of ANGPTL3 lowering.

Interestingly, the association of ANGPTL3 inactivation with CAD was only present for rare LoF variants when the carrier status was determined by DNA sequencing. This exposes the limitations of drug-target MR studies using DNA micro-array-based GWAS. When rare variants are incorrectly imputed, this typically introduces a one-sided loss of information that biases toward the null hypothesis, leading to falsely negative findings (49). Even though the imputation quality score (e.g., 'INFO') reports an imputation quality metric, this metric does not really measure the true imputation accuracy (57). The imputation accuracy can only truly be determined if variant carrier status is called by genotyping (e.g., via DNA sequencing). However, studying rare variants in genetic association studies is not without drawbacks. An important limitation of the use of rare variants is statistical imprecision simply due to their rarity (55). Rare variants also often emerged relatively recently and consequently are more susceptible to confounding by enrichment in specific geographical regions, families, or socioeconomic strata (56). Even if appropriate model adjustments are applied, subtle differences in population structure could cause a small number of extra alleles to be present in the control (or case) group. This can lead to biased estimates when the rare alternative allele is present in ten, or hundred individuals in total, which is often the case for rare variant studies even when the total sample size is above hundreds of thousands. Overall, our findings underscore the importance of combining evidence from exome sequencing and common variants in genetic association studies of complex disease phenotypes.

Compared to clinical trials, MR analysis can exaggerate the magnitude of the effect of inactivating a gene/protein (58). This is because MR and other genetic association studies estimate lifelong exposure to changed gene function, while drug trials typically last 2–5 years in late adulthood. If the treatment effect multiplicatively interacts with time, MR may exaggerate it. This constraint should be considered when translating MR findings to predict the results of clinical trials. For ANGPTL4, Dewey et al. (50), found that the TG levels of p.E40K homozygotes were reduced by 0.58 mmol/L (0.92 mmol/L for p.E40K homozygotes vs. 1.49 mmol/L in non-carriers; relative change -39%) in a normotriglyceridemic population. When translating these findings (TG reduction of 0.58 mmol/L) onto the effect size on CAD found in this study, one would expect that lifetime *ANGPTL4* inactivation—in a population of normotriglyceridemic individuals—results in a risk reduction corresponding to a CAD odds ratio of 0.61 (95% CI: 0.52–0.72).

In conclusion, our genetic analysis predicts that in a broader dyslipidemic patient population, therapies aimed at decreasing plasma ANGPTL3, ANGPTL4, or APOC3 levels will be effective in preventing

486 CAD without raising specific safety concerns. In addition, therapies aimed at reducing plasma levels of
487 ANGPTL4 may provide additional benefits to patients with dyslipidemia and T2D.

ETHICAL REVIEW

This study analyzed scientific data that is available to the public, as detailed in **Table 1** and **Supplemental Table 1**, where references to the specific datasets can be found. Ethical oversight was conducted by review boards, ensuring that all studies complied with the ethical standards outlined in the Helsinki Declaration.

ACKNOWLEDGEMENTS

We would like to thank the participants and researchers of the CARDIoGRAMplusC4D, CKDGen, deCODE, DIAGRAM, EPIC-CVD, FinnGen, GIGASTROKE, GLGC, and UK biobank studies, as well as the other non-consortium studies.

FUNDING

This research received no specific grants from public or non-profit funding agencies.

CONFLICT OF INTEREST

F.L. is a part-time employee of Lipigon Pharmaceuticals AB. S.K.N. is the chief executive officer of Lipigon. S.K. is a paid consultant for Lipigon.

DATA AVAILABILITY STATEMENT

Database identifiers and links to the data sets are provided in **Supplemental Table 1**. The analyses in this manuscript were performed using the R programming language (v.4.2.1) with the packages coloc, cowplot, data.table, ggplot2, ggthemes, mungegwas, phewas, twosamplemr, wesanderson, writexl, and the Python programming language (v.3.8.16) using the packages numpy, pandas, and scipy. The LD matrix estimates were calculated using PLINK (v1.90b6.24).

508 **REFERENCES**

509 1. Tardif JC, Karwatowska-Prokopczuk E, Amour ES, Ballantyne CM, Shapiro MD, Moriarty
510 PM, et al. Apolipoprotein C-III reduction in subjects with moderate hypertriglyceridaemia and at high
511 cardiovascular risk. Eur Heart J. 2022;43(14):1401-12.
512 2. Ahmad Z, Banerjee P, Hamon S, Chan KC, Bouzelmat A, Sasiela WJ, et al. Inhibition of
513 Angiopoietin-Like Protein 3 With a Monoclonal Antibody Reduces Triglycerides in
514 Hypertriglyceridemia. Circulation. 2019;140(6):470-86.
515 3. Dewey FE, Gusarova V, Dunbar RL, O'Dushlaine C, Schurmann C, Gottesman O, et al.
516 Genetic and Pharmacologic Inactivation of ANGPTL3 and Cardiovascular Disease. N Engl J Med.
517 2017;377(3):211-21.
518 4. Gaudet D, Gipe DA, Pordy R, Ahmad Z, Cuchel M, Shah PK, et al. ANGPTL3 Inhibition in
519 Homozygous Familial Hypercholesterolemia. N Engl J Med. 2017;377(3):296-7.
520 5. Raal FJ, Rosenson RS, Reeskamp LF, Hovingh GK, Kastelein JJP, Rubba P, et al.
521 Evinacumab for Homozygous Familial Hypercholesterolemia. N Engl J Med. 2020;383(8):711-20.
522 6. Rosenson RS, Burgess LJ, Ebenbichler CF, Baum SJ, Stroes ESG, Ali S, et al. Evinacumab in
523 Patients with Refractory Hypercholesterolemia. N Engl J Med. 2020;383(24):2307-19.
524 7. Gaudet D, Karwatowska-Prokopczuk E, Baum SJ, Hurh E, Kingsbury J, Bartlett VJ, et al.
525 Vupanorsen, an N-acetyl galactosamine-conjugated antisense drug to ANGPTL3 mRNA, lowers
526 triglycerides and atherogenic lipoproteins in patients with diabetes, hepatic steatosis, and
527 hypertriglyceridaemia. Eur Heart J. 2020;41(40):3936-45.
528 8. Graham MJ, Lee RG, Brandt TA, Tai LJ, Fu W, Peralta R, et al. Cardiovascular and Metabolic
529 Effects of ANGPTL3 Antisense Oligonucleotides. N Engl J Med. 2017;377(3):222-32.
530 9. Watts GF, Schwabe C, Scott R, Gladding P, Sullivan D, Baker J, et al. Abstract 15751:
531 Pharmacodynamic Effect of ARO-ANG3, an Investigational RNA Interference Targeting Hepatic
532 Angiopoietin-like Protein 3, in Patients With Hypercholesterolemia. Circulation.
533 2020;142(Suppl_3):A15751-A.
534 10. Bergmark BA, Marston NA, Bramson CR, Curto M, Ramos V, Jevne A, et al. Effect of
535 Vupanorsen on Non-High-Density Lipoprotein Cholesterol Levels in Statin-Treated Patients With
536 Elevated Cholesterol: TRANSLATE-TIMI 70. Circulation. 2022;145(18):1377-86.
537 11. Reeskamp LF, Nurmohamed NS, Bom MJ, Planken RN, Driessen RS, van Diemen PA, et al.
538 Marked plaque regression in homozygous familial hypercholesterolemia. Atherosclerosis.
539 2021;327:13-7.
540 12. Khoury E, Lauzière A, Raal FJ, Mancini J, Gaudet D. Atherosclerotic plaque regression in
541 homozygous familial hypercholesterolaemia: a case report of a long-term lipid-lowering therapy
542 involving LDL-receptor-independent mechanisms. Eur Heart J Case Rep. 2023;7(1):ytad029.

543 13. Desai U, Lee EC, Chung K, Gao C, Gay J, Key B, et al. Lipid-lowering effects of anti-
544 angiopoietin-like 4 antibody recapitulate the lipid phenotype found in angiopoietin-like 4 knockout
545 mice. Proc Natl Acad Sci U S A. 2007;104(28):11766-71.
546 14. Lichtenstein L, Mattijssen F, de Wit NJ, Georgiadi A, Hooiveld GJ, van der Meer R, et al.
547 Angptl4 protects against severe proinflammatory effects of saturated fat by inhibiting fatty acid uptake
548 into mesenteric lymph node macrophages. Cell Metab. 2010;12(6):580-92.
549 15. Oteng AB, Bhattacharya A, Brodesser S, Qi L, Tan NS, Kersten S. Feeding Angptl4-/- mice
550 trans fat promotes foam cell formation in mesenteric lymph nodes without leading to ascites. J Lipid
551 Res. 2017;58(6):1100-13.
552 16. Deng M, Kutrolli E, Sadewasser A, Michel S, Joibari MM, Jaschinski F, et al. ANGPTL4
553 silencing via antisense oligonucleotides reduces plasma triglycerides and glucose in mice without
554 causing lymphadenopathy. J Lipid Res. 2022;63(7):100237.
555 17. Ferkingstad E, Sulem P, Atlason BA, Sveinbjornsson G, Magnusson MI, Styrmisdottir EL, et
556 al. Large-scale integration of the plasma proteome with genetics and disease. Nat Genet.
557 2021;53(12):1712-21.
558 18. Dhindsa RS, Burren OS, Sun BB, Prins BP, Matelska D, Wheeler E, et al. Rare variant
559 associations with plasma protein levels in the UK Biobank. Nature. 2023;622(7982):339-47.
560 19. Wang Q, Dhindsa RS, Carss K, Harper AR, Nag A, Tachmazidou I, et al. Rare variant
561 contribution to human disease in 281,104 UK Biobank exomes. Nature. 2021;597(7877):527-32.
562 20. Kurki MI, Karjalainen J, Palta P, Sipilä TP, Kristiansson K, Donner KM, et al. FinnGen
563 provides genetic insights from a well-phenotyped isolated population. Nature. 2023;613(7944):508-18.
564 21. Sudlow C, Gallacher J, Allen N, Beral V, Burton P, Danesh J, et al. UK biobank: an open
565 access resource for identifying the causes of a wide range of complex diseases of middle and old age.
566 PLoS Med. 2015;12(3):e1001779.
567 22. Aragam KG, Jiang T, Goel A, Kanoni S, Wolford BN, Atri DS, et al. Discovery and
568 systematic characterization of risk variants and genes for coronary artery disease in over a million
569 participants. Nat Genet. 2022;54(12):1803-15.
570 23. Wuttke M, Li Y, Li M, Sieber KB, Feitosa MF, Gorski M, et al. A catalog of genetic loci
571 associated with kidney function from analyses of a million individuals. Nat Genet. 2019;51(6):957-72.
572 24. Mishra A, Malik R, Hachiya T, Jürgenson T, Namba S, Posner DC, et al. Stroke genetics
573 informs drug discovery and risk prediction across ancestries. Nature. 2022;611(7934):115-23.
574 25. Ghodsian N, Abner E, Emdin CA, Gobeil É, Taba N, Haas ME, et al. Electronic health record-
575 based genome-wide meta-analysis provides insights on the genetic architecture of non-alcoholic fatty
576 liver disease. Cell Rep Med. 2021;2(11):100437.
577 26. Mahajan A, Taliun D, Thurner M, Robertson NR, Torres JM, Rayner NW, et al. Fine-mapping
578 type 2 diabetes loci to single-variant resolution using high-density imputation and islet-specific
579 epigenome maps. Nat Genet. 2018;50(11):1505-13.

27. Nag A, Dhindsa RS, Middleton L, Jiang X, Vitsios D, Wigmore E, et al. Effects of protein-coding variants on blood metabolite measurements and clinical biomarkers in the UK Biobank. Am J Hum Genet. 2023;110(3):487-98.
28. Evangelou E, Warren HR, Mosen-Ansorena D, Mifsud B, Pazoki R, Gao H, et al. Genetic analysis of over 1 million people identifies 535 new loci associated with blood pressure traits. Nat Genet. 2018;50(10):1412-25.
29. Pulit SL, Stoneman C, Morris AP, Wood AR, Glastonbury CA, Tyrrell J, et al. Meta-analysis of genome-wide association studies for body fat distribution in 694 649 individuals of European ancestry. Hum Mol Genet. 2019;28(1):166-74.
30. Elsworth B, Lyon M, Alexander T, Liu Y, Matthews P, Hallett J, et al. The MRC IEU OpenGWAS data infrastructure. bioRxiv. 2020:2020.08.10.244293.
31. Stanzick KJ, Li Y, Schlosser P, Gorski M, Wuttke M, Thomas LF, et al. Discovery and prioritization of variants and genes for kidney function in >1.2 million individuals. Nat Commun. 2021;12(1):4350.
32. Liu Y, Basty N, Whitcher B, Bell JD, Sorokin EP, van Bruggen N, et al. Genetic architecture of 11 organ traits derived from abdominal MRI using deep learning. Elife. 2021;10.
33. Burgess S, Dudbridge F, Thompson SG. Combining information on multiple instrumental variables in Mendelian randomization: comparison of allele score and summarized data methods. Stat Med. 2016;35(11):1880-906.
34. Schmidt AF, Finan C, Gordillo-Marañón M, Asselbergs FW, Freitag DF, Patel RS, et al. Genetic drug target validation using Mendelian randomisation. Nat Commun. 2020;11(1):3255.
35. Slatkin M. Linkage disequilibrium--understanding the evolutionary past and mapping the medical future. Nat Rev Genet. 2008;9(6):477-85.
36. Zuber V, Grinberg NF, Gill D, Manipur I, Slob EAW, Patel A, et al. Combining evidence from Mendelian randomization and colocalization: Review and comparison of approaches. Am J Hum Genet. 2022;109(5):767-82.
37. Giambartolomei C, Vukcevic D, Schadt EE, Franke L, Hingorani AD, Wallace C, et al. Bayesian test for colocalisation between pairs of genetic association studies using summary statistics. PLoS Genet. 2014;10(5):e1004383.
38. McLaren W, Gil L, Hunt SE, Riat HS, Ritchie GR, Thormann A, et al. The Ensembl Variant Effect Predictor. Genome Biol. 2016;17(1):122.
39. Abraham W. The Fitting of Straight Lines if Both Variables are Subject to Error. The Annals of Mathematical Statistics. 1940;11(3):284-300.
40. Landfors F, Chorell E, Kersten S. Genetic Mimicry Analysis Reveals the Specific Lipases Targeted by the ANGPTL3-ANGPTL8 Complex and ANGPTL4. J Lipid Res. 2023;64(1):100313.

615 41. Wang Q, Oliver-Williams C, Raitakari OT, Viikari J, Lehtimaki T, Kahonen M, et al.
616 Metabolic profiling of angiopoietin-like protein 3 and 4 inhibition: a drug-target Mendelian
617 randomization analysis. Eur Heart J. 2021;42(12):1160-9.
618 42. Yin W, Romeo S, Chang S, Grishin NV, Hobbs HH, Cohen JC. Genetic variation in
619 ANGPTL4 provides insights into protein processing and function. J Biol Chem. 2009;284(19):13213-
620 22.
621 43. Richardson TG, Leyden GM, Wang Q, Bell JA, Elsworth B, Davey Smith G, et al.
622 Characterising metabolomic signatures of lipid-modifying therapies through drug target mendelian
623 randomisation. PLoS Biol. 2022;20(2):e3001547.
624 44. Stitziel NO, Khera AV, Wang X, Bierhals AJ, Vourakis AC, Sperry AE, et al. ANGPTL3
625 Deficiency and Protection Against Coronary Artery Disease. J Am Coll Cardiol. 2017;69(16):2054-63.
626 45. Musunuru K, Pirruccello JP, Do R, Peloso GM, Guiducci C, Sougnez C, et al. Exome
627 sequencing, ANGPTL3 mutations, and familial combined hypolipidemia. N Engl J Med.
628 2010;363(23):2220-7.
629 46. Rivas MA, Pirinen M, Conrad DF, Lek M, Tsang EK, Karczewski KJ, et al. Human genomics.
630 Effect of predicted protein-truncating genetic variants on the human transcriptome. Science.
631 2015;348(6235):666-9.
632 47. Kovrov O, Kristensen KK, Larsson E, Ploug M, Olivecrona G. On the mechanism of
633 angiopoietin-like protein 8 for control of lipoprotein lipase activity. J Lipid Res. 2019;60(4):783-93.
634 48. Cherukuri PF, Soe MM, Condon DE, Bartaria S, Meis K, Gu S, et al. Establishing analytical
635 validity of BeadChip array genotype data by comparison to whole-genome sequence and standard
636 benchmark datasets. BMC Med Genomics. 2022;15(1):56.
637 49. Stahl K, Gola D, König IR. Assessment of Imputation Quality: Comparison of Phasing and
638 Imputation Algorithms in Real Data. Front Genet. 2021;12:724037.
639 50. Dewey FE, Gusarova V, O'Dushlaine C, Gottesman O, Trejos J, Hunt C, et al. Inactivating
640 Variants in ANGPTL4 and Risk of Coronary Artery Disease. N Engl J Med. 2016;374(12):1123-33.
641 51. Jorgensen AB, Frikke-Schmidt R, Nordestgaard BG, Tybjaerg-Hansen A. Loss-of-function
642 mutations in APOC3 and risk of ischemic vascular disease. N Engl J Med. 2014;371(1):32-41.
643 52. Gusarova V, Alexa CA, Wang Y, Rafique A, Kim JH, Buckler D, et al. ANGPTL3 blockade
644 with a human monoclonal antibody reduces plasma lipids in dyslipidemic mice and monkeys. J Lipid
645 Res. 2015;56(7):1308-17.
646 53. Thomas DG, Wei Y, Tall AR. Lipid and metabolic syndrome traits in coronary artery disease:
647 a Mendelian randomization study. J Lipid Res. 2021;62:100044.
648 54. Singaraja RR, Sivapalaratnam S, Hovingh K, Dubé MP, Castro-Perez J, Collins HL, et al. The
649 impact of partial and complete loss-of-function mutations in endothelial lipase on high-density
650 lipoprotein levels and functionality in humans. Circ Cardiovasc Genet. 2013;6(1):54-62.

651 55. Zuk O, Schaffner SF, Samocha K, Do R, Hechter E, Kathiresan S, et al. Searching for missing
652 heritability: designing rare variant association studies. Proc Natl Acad Sci U S A. 2014;111(4):E455-
653 64.
654 56. Locke AE, Steinberg KM, Chiang CWK, Service SK, Havulinna AS, Stell L, et al. Exome
655 sequencing of Finnish isolates enhances rare-variant association power. Nature. 2019;572(7769):323-
656 8.
657 57. Zheng HF, Rong JJ, Liu M, Han F, Zhang XW, Richards JB, et al. Performance of genotype
658 imputation for low frequency and rare variants from the 1000 genomes. PLoS One.
659 2015;10(1):e0116487.
660 58. Burgess S, Butterworth A, Malarstig A, Thompson SG. Use of Mendelian randomisation to
661 assess potential benefit of clinical intervention. BMJ. 2012;345:e7325.

662

APPENDICES

Supplemental Note

In-depth information regarding diagnostic criteria for diseases, definitions of continuous outcomes, and sensitivity analyses. The supplemental note .docx also contains Supplemental Figures 1-5.

Supplemental Figures

The Supplemental Figures 1-5 are contained within the supplemental note .docx file.

Figure S1. Scatter plots showing the results of the drug-target MR analyses.

Each subplot represents the results of the analyses displayed in **Figures 1-3** of the main manuscript.

Figure S2. Regional genetic association plots displaying the results of the colocalization analyses.

Each subplot represents the results of the analyses displayed in **Figures 1-3** of the main manuscript.

Figure S3. Results of cis-pQTL MR analyses of the estimated glomerular filtration rate by (eGFR) by Cystatin C and plasma Creatinine.

The findings are displayed in bar graphs, showing the effect per s.d. decrease in protein abundance. The red lines represent the 95% CI.

Figure S4. Results of phenome-wide MR analysis on FinnGen outcomes using ANGPTL3 rs34483103-1:62604866:AGTTAATGTG>A [3 prime UTR, c.*52_*60del] and APOC3 rs138326449-11:116830638:G>A [donor loss, c.55+1G>A] variants.

A: Volcano plot displaying the results of ANGPTL3 cis-pQTL phenome-wide MR. B: APOC3 cis-pQTL phenome-wide MR volcano plot. The y-axis solid straight lines indicate the phenome-wide significance threshold. 'OR' indicates the odds ratio with 95% confidence intervals with Bonferroni correction for the 694 FinnGen outcomes.

Figure S5. Results of functional variant triglycerides-mediated CAD MR analyses of ANGPTL3 and ANGPTL4.

Forest plot and table displaying the results of the CAD MR analyses limiting instrument selection to functional variants in ANGPTL3 and ANGPTL4.

Supplemental Tables

The Supplemental Tables 1-9 are located within the Supplemental Tables .xlsx file.

Supplemental Table 1. Description of GWAS data sets

List of the GWAS data sets used. 'database.ID' denotes the EBI GWAS catalog identifiers if starting by "GCST", or the UK biobank showcase identifier if starting by a number.

Supplemental Table 2. MR results with 1000Genomes LD matrix

Results of the MR analyses that are presented in the paper. 'rsids.dbsnp.ver144' denote the rsids that were used in each MR model.

Supplemental Table 3. MR sensitivity analysis w. UKB 337K LD matrix vs 1000Genomes.

LD matrix sensitivity analysis using the 1000Genomes and UKB 337K LD matrices. 'het.beta' indicates whether the coefficients directionality differed between the two settings. 'heterogeneity.statistic' indicates the heterogeneity P-value, which is described in detail in the supplemental note.

Supplemental Table 4. MR sample overlap risk of bias analysis

Result of the risk of bias from sample overlap analysis reporting the F-statistics, bias ('Beta.bias.low.scenario', ' Beta.bias.medium.scenario', and ' Beta.bias.high.scenario') and type 1 error inflation (Type1error.lowbias.scenario, Type1error.mediumbias.scenario, Type1error.highbias.scenario) for each scenario and model.

Supplemental Table 5. ICD codes used for UKB lymphadenopathy-related phecodes

Phecode and ICD-codes as described in the Methods section.

Supplemental Table 6. ANGPTL4 p.40K pQTL MR PheWAS results

Detailed results of the MR analyses presented in **Figure 3D**.

Supplemental Table 7. ANGPTL4 p.Cys80fs pQTL MR PheWAS results

Detailed results of the MR analyses presented in **Figure 3D**.

Supplemental Table 8. ***ANGPTL3 rs34483103-1:62604866:AGTTAATGTG>A*** **[3 prime UTR, c.*52_*60del]pQTL MR PheWAS results**

Detailed results of the MR analyses presented in **Supplemental Figure 3A**.

Supplemental Table 9. ***APOC3 rs138326449-11:116830638:G>A*** **[donor loss, c.55+1G>A]pQTL MR PheWAS results**

Detailed results of the MR analyses presented in **Supplemental Figure 3B**.